ARMY RESEARCH LABORATORY

Computational Fluid Dynamics Results for a 25-mm Projectile

by Karen Heavey and Jubaraj Sahu

ARL-MR-676 **September 2007**

NOTICES

Disclaimers

The findings in this report are not to be construed as an official Department of the Army position unless so designated by other authorized documents.

Citation of manufacturer's or trade names does not constitute an official endorsement or approval of the use thereof.

Destroy this report when it is no longer needed. Do not return it to the originator.

Army Research Laboratory
Aberdeen Proving Ground, MD 21005-5066

ARL-MR-676 **September 2007**

Computational Fluid Dynamics Results for a 25-mm Projectile

Karen Heavey and Jubaraj Sahu
Weapons and Materials Research Directorate, ARL

REPORT DOCUMENTATION PAGE	Form Approved OMB No. 0704-0188

1. REPORT DATE *(DD-MM-YYYY)*	2. REPORT TYPE	3. DATES COVERED (From - To)
September 2007	Final	November 2005–June 2006

4. TITLE AND SUBTITLE
Computational Fluid Dynamics Results for a 25-mm Projectile

5a. CONTRACT NUMBER

5b. GRANT NUMBER

5c. PROGRAM ELEMENT NUMBER

6. AUTHOR(S)
Karen Heavey and Jubaraj Sahu

5d. PROJECT NUMBER
622618AH80

5e. TASK NUMBER

5f. WORK UNIT NUMBER

7. PERFORMING ORGANIZATION NAME(S) AND ADDRESS(ES)
U.S. Army Research Laboratory
ATTN: AMSRD-ARL-WM-BC
Aberdeen Proving Ground, MD 21005-5066

8. PERFORMING ORGANIZATION REPORT NUMBER
ARL-MR-676

9. SPONSORING/MONITORING AGENCY NAME(S) AND ADDRESS(ES)

10. SPONSOR/MONITOR'S ACRONYM(S)

11. SPONSOR/MONITOR'S REPORT NUMBER(S)

12. DISTRIBUTION/AVAILABILITY STATEMENT
Approved for public release; distribution is unlimited.

13. SUPPLEMENTARY NOTES

14. ABSTRACT
Computational fluid dynamics approaches were used to compute the flow fields of a 25-mm projectile, modeled with and without a jet cavity. Steady-state numerical results have been obtained for a series of cases at Mach number 0.756, at 0° angle of attack, with jet pressures of 3, 6, and 12 atm. Full three-dimensional computations were performed using a two-equation realizable k-ε turbulence model. Force and moment data have been extracted from the solutions for comparison and show that increasing jet pressure increases the effect on normal force and pitching moment while having little effect on drag.

15. SUBJECT TERMS
baseline, computational fluid dynamics, guided projectile, jet cavity

16. SECURITY CLASSIFICATION OF:			17. LIMITATION OF ABSTRACT	18. NUMBER OF PAGES	19a. NAME OF RESPONSIBLE PERSON
a. REPORT	b. ABSTRACT	c. THIS PAGE			Karen R. Heavey
UNCLASSIFIED	UNCLASSIFIED	UNCLASSIFIED	UL	24	19b. TELEPHONE NUMBER (*Include area code*) 410-306-0793

Standard Form 298 (Rev. 8/98)
Prescribed by ANSI Std. Z39.18

Contents

List of Figures iv

List of Tables iv

Acknowledgments v

1. Introduction 1

2. Solution Technique 1

2.1 CFD++ Flow Solver 1

2.2 Numerical Technique 2

3. Model Geometry and Numerical Grid 3

3.1 Projectile Model and Geometry 3

3.2 Computational Mesh 3

4. Results and Discussion 4

4.1 Qualitative Results 5

4.2 Quantitative Results 7

5. Summary and Conclusions 12

6. References 13

Distribution List 14

List of Figures

Figure 1. Computational model of a 25-mm projectile with jet cavity (top view). 3
Figure 2. Surface grid, view from the side....4
Figure 3. Computation mesh showing the intersection of the body and jet cavity. 4
Figure 4. Computation mesh, axisymmetric view showing internal cavity. 5
Figure 5. Surface pressure contours on the baseline projectile. 6
Figure 6. Flowfield pressure contours on the baseline projectile. 6
Figure 7. Mach contours for the baseline projectile. 7
Figure 8. Mach contours for various jet pressures: 3, 6, and 12 atm (top to bottom). 8
Figure 9. Expanded view of pressure contours for various jet pressures: 3, 6, and 12 atm (top to bottom). 9
Figure 10. Expanded view of surface pressure contours for various jet pressures: 3, 6, and 12 atm (top to bottom). 10
Figure 11. CFD++ results for normal force. 11

List of Tables

Table 1. Computed values for normal force. 11
Table 2. Computed aerodynamic coefficients. 11

Acknowledgments

The authors would like to thank Georgia Tech for providing the computer-aided design files for the projectile models. The computational support of the U.S. Army Research Laboratory Major Shared Resource Center is also greatly appreciated.

INTENTIONALLY LEFT BLANK.

1. Introduction

The prediction of aerodynamic coefficients for projectile configurations is essential in assessing the performance of new designs. Accurate determination of aerodynamics is critical to the low-cost development of new advanced guided projectiles, rockets, missiles, and smart munitions. Fins, canards, and jets can be used to provide control for maneuvering projectiles and missiles. The flow fields associated with these control mechanisms for the modern weapons are complex and involve three-dimensional (3-D) shock-boundary layer interactions and highly viscous dominated separated flow regions (*1*). Computational fluid dynamics (CFD) has emerged as a critical technology for the aerodynamic design and assessment of weapons. Improved computer technology and state-of-the-art numerical procedures enable solutions to complex 3-D problems associated with projectile and missile aerodynamics. In general, these techniques produce accurate and reliable numerical results for simple projectile and missile configurations at small angles of attack.

The information presented in this U.S. Army Research Laboratory (ARL) report focuses on a 25-mm projectile, with and without a jet cavity. A description of the computational techniques is presented, followed by a description of the application of these techniques to both configurations. Computed results for both models are presented at a Mach number 0.756 at 0° angle of attack, with the jet off. Additional results using jet pressures of 3, 6, and 12 atm are presented for the model with the cavity (jet on).

2. Solution Technique

2.1 CFD++ Flow Solver

A commercially available code, CFD++ (*2*, *3*), is used for the numerical simulations. The basic numerical framework in the code contains unified-grid, unified-physics, and unified-computing features. The reader is directed to the references for details, as only a brief synopsis of the methodology is supplied in this report.

The 3-D, Reynolds-averaged Navier-Stokes (*4*) equations are solved using the following finite volume method:

$$\frac{\partial}{\partial t}\int_V \mathbf{W} dV + \oint \left[\mathbf{F} - \mathbf{G}\right] \cdot dA = \int_V \mathbf{H} dV, \tag{1}$$

where **W** is the vector of conservative variables, **F** and **G** are the inviscid and viscous flux vectors, respectively, **H** is the vector of source terms, V is the cell volume, and A is the surface area of the cell face.

The numerical framework of CFD++ is based on the following general elements: (1) unsteady compressible and incompressible Navier-Stokes equations with turbulence modeling (unified-physics); (2) unification of Cartesian, structured curvilinear, and unstructured grids, including hybrids (unified-grid); (3) unification of treatment of various cell shapes including hexahedral, tetrahedral and triangular prism cells (3-D), quadrilateral and triangular cells (two-dimensional), and linear elements (one-dimensional) (unified-grid); (4) treatment of multiblock patched aligned (nodally connected), patched-nonaligned, and overset grids (unified-grid); (5) total variation diminishing discretization based on a new multidimensional interpolation framework; (6) Riemann solvers to provide proper signal propagation physics, including versions for preconditioned forms of the governing equations; (7) consistent and accurate discretization of viscous terms using the same multidimensional polynomial framework; (8) pointwise turbulence models that do not require knowledge of distance to walls; (9) versatile boundary condition implementation that includes a rich variety of integrated boundary condition types for the various sets of equations; (10) implementation on massively parallel computers based on the distributed-memory message-passing model using native message-passing libraries or MPI, PVM, etc. (unified-computing).

The code has brought together several ideas on convergence acceleration to yield a fast methodology for all flow regimes. The approach can be labeled as a preconditioned-implicit-relaxation scheme. It combines three basic ideas—implicit local time-stepping, relaxation, and preconditioning. Preconditioning the equations ideally equalizes the eigen values of the inviscid flux Jacobians and removes the stiffness arising from large discrepancies between the flow and sound velocities at low speeds. Use of an implicit scheme circumvents the stringent stability limits suffered by their explicit counterparts, and successive relaxation allows update of cells as information becomes available and thus aids convergence.

2.2 Numerical Technique

The two-equation realizable k-ε turbulence model was selected for this study. For boundary conditions, an isothermal wall condition was used on the projectile surface and a characteristics-based inflow/outflow routine was used for the farfield boundary. An inflow boundary condition using preselected velocities was used for the jet. Calculations were performed under the following free-stream wind tunnel conditions: Mach number = 0.756, Tinf = 258.9 K, and Pinf = 66536.75 N/m^2.

All computations were performed on the IBM SP-4 at the ARL Major Shared Resource Center. Most of the cases were completed utilizing 16 processors per run and averaged 100 CPU hours to converge. The next section describes the model geometries and the computational mesh.

3. Model Geometry and Numerical Grid

3.1 Projectile Model and Geometry

In this study, two projectile configurations are considered. The geometric model for the baseline case is a 25-mm projectile (*5*), and the length of the projectile is 89 mm. The model was modified by adding a cylindrical jet cavity on the top surface of the projectile. The diameter of the jet cavity is 1.2 mm; the center of the jet cavity is located 52 mm from the nose. Figure 1 is view of the top of the projectile showing the surface location of the jet cavity. The cavity is 11.25 mm deep.

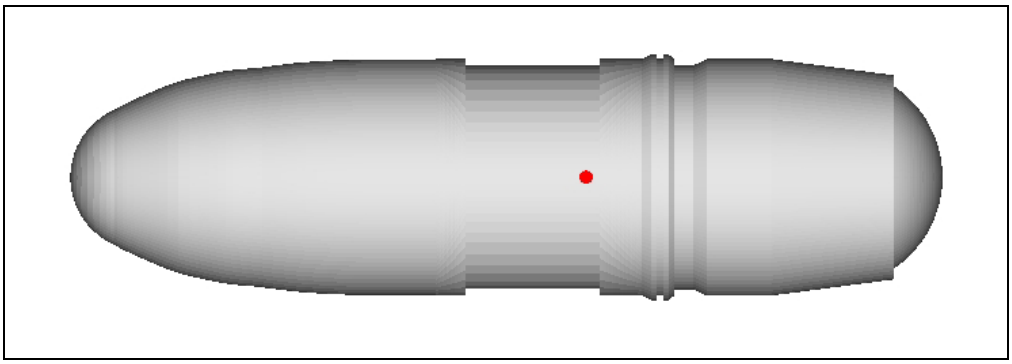

Figure 1. Computational model of a 25-mm projectile with jet cavity (top view).

3.2 Computational Mesh

The grids for the computational models were created using GRIDGEN (*6*), a commercially available software package. A computer-aided design file supplied by Georgia Tech served as a starting point to provide the basic geometry. Using a variable blocking strategy, a structured hexahedral mesh was created. The grid for the baseline projectile consisted of 4.4-million hexahedral cells, with the outer boundary extending approximately 20 body lengths from the projectile surface. Figure 2 shows the surface grid on the projectile as seen from the side. Several iterations were required to generate the mesh for the model with the jet cavity. An additional mesh was generated to model the cavity, and the density of the original surface mesh was increased in this area. The final grid configuration for the projectile with the cavity consisted of 6.2-million grid points. The intersection of these two grids (on the top surface of the projectile) is shown in figure 3. The application of zonal boundary conditions to this intersection allows for the transfer of data between the two grids. An axisymmetric cut of the computational mesh (figure 4) shows the cavity grid in the interior of the projectile. This figure also shows the grid density in the boundary layer region and in the area of the jet exit as well.

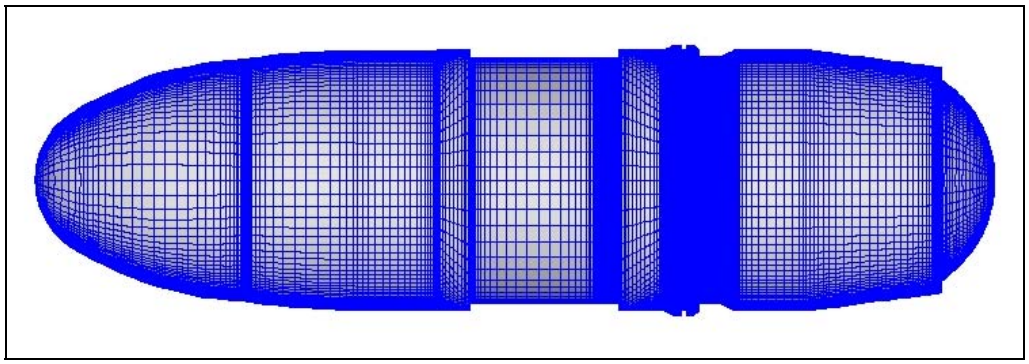

Figure 2. Surface grid, view from the side.

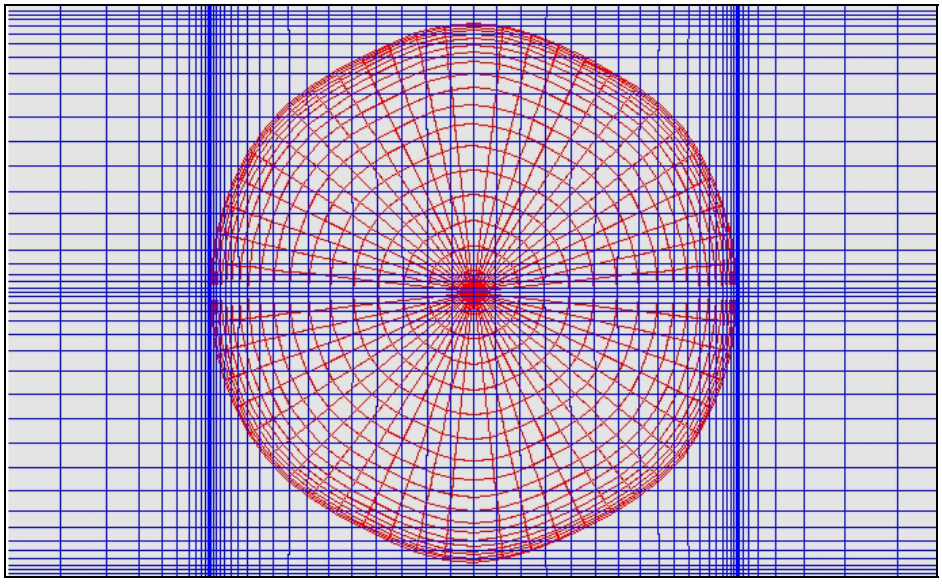

Figure 3. Computation mesh showing the intersection of the body and jet cavity.

4. Results and Discussion

Computations using viscous Navier-Stokes methods were performed to predict the flow field and aerodynamic coefficients for a 25-mm projectile, with and without jet, using the CFD++ flow solver. Run parameters are Mach number 0.756, alpha 0, with jet pressures of 0, 3, 6, and 12 atm. Full 3-D calculations were performed, and no symmetry was used. Force and moment data were extracted from the computational results.

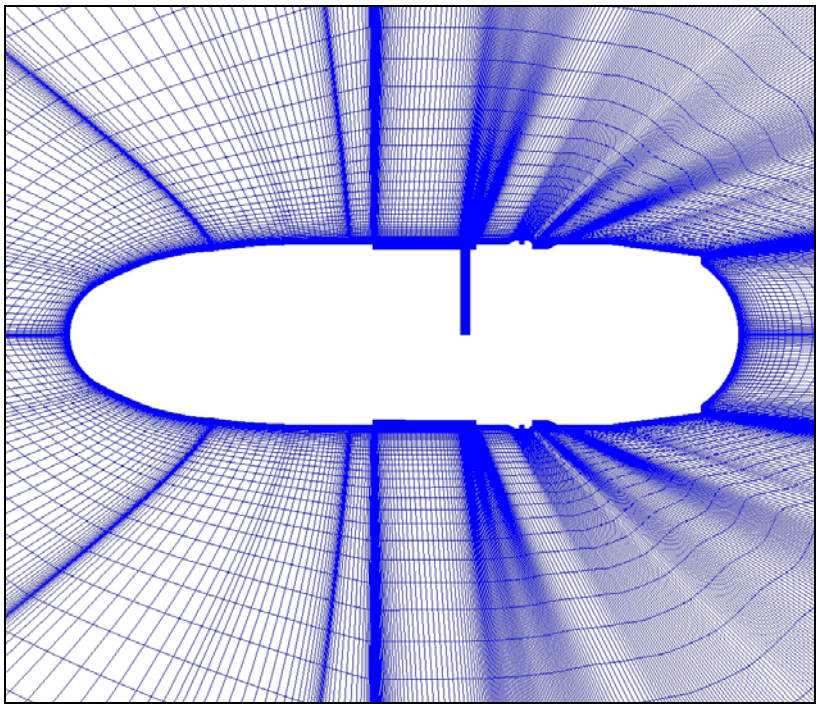

Figure 4. Computation mesh, axisymmetric view showing internal cavity.

4.1 Qualitative Results

Figure 5 shows surface pressure contours on the baseline model. There is an area of high pressure on the nose on the projectile. Over a series of cuts and rotating bands, changes in pressure vary along the surface of the projectile. Pressure and mach contours for the symmetry plane (figures 6 and 7) show the flowfield to be axisymmetric and typical for a projectile at 0° angle of attack at a low transonic speed. These figures again show high pressure (or low velocity) regions in front of the projectile. A region of low pressure can be seen on the nose-section near the nose-cylinder junction of the projectile and in the vicinity of the rotating bands. The low-speed region, as identified in blue, is evident in the near wake (figure 7).

The next series of figures show Mach contours and pressure contours for various jet pressures applied to a single projectile model.

Figure 8 shows Mach contours in the symmetry plane for the three jet pressures—3 atm at the top, 6 atm for the middle, and 12 atm at the bottom graphic. With increasing jet pressure, the interaction of the jet with the free-stream flowfield gets stronger. The extent of jet interaction is evident in the flowfield downstream of the jet location on the leeside of the projectile. There is a slight asymmetry in the near wake flowfield for the highest jet pressure of 12 atm. The flowfield in front of the jet is largely unaffected by the presence of the jet.

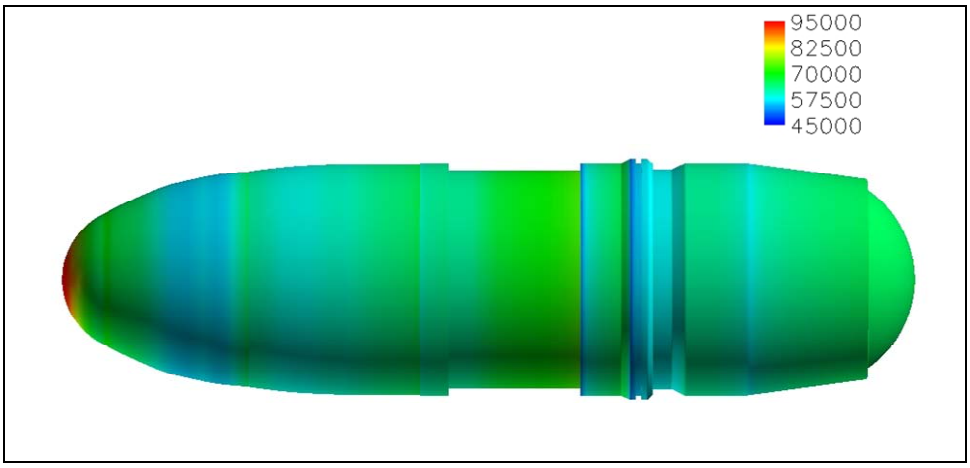

Figure 5. Surface pressure contours on the baseline projectile.

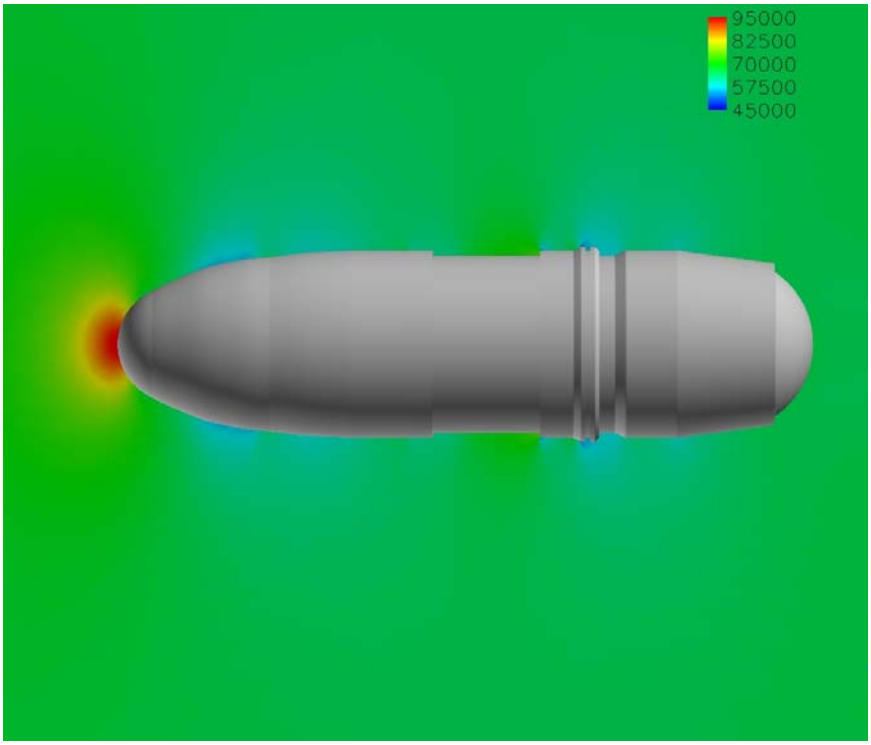

Figure 6. Flowfield pressure contours on the baseline projectile.

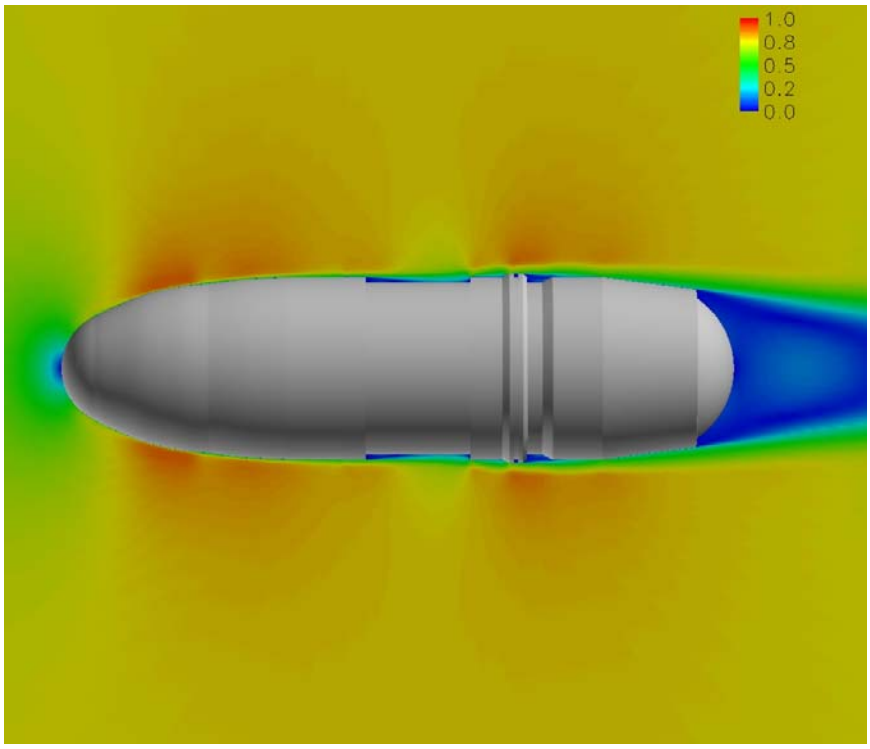

Figure 7. Mach contours for the baseline projectile.

Figure 9 shows pressure contours in the symmetry plane in the vicinity of the jet. As the pressure of the jet increases (top to bottom), the area of high pressure in front of the jet increases, and the area of low pressure behind the jet increases also. This same effect is observed on the surface of the projectile (as shown in figure 10), which shows the surface pressure in the vicinity of the jet. Again, the stronger the jet pressure, the larger the effect on the flowfield downstream of the jet, in the axial and the circumferential directions. The effect upstream is small.

4.2 Quantitative Results

Using the tools provided in the CFD++ software, force and moment data were extracted from the flowfield solutions. The effect of jet pressure on normal force is shown graphically in figure 11. These computed values are also presented in tabular form (table 1). These results show that a stronger jet has a larger effect on the normal force.

Various aerodynamic coefficients are presented in table 2. The jet appears to have no effect on projectile drag (CX). Although the model without the cavity has a slightly higher drag value, this is most likely due to the difference in the computational mesh described earlier. The other two coefficients presented, normal force (CN) and pitching moment (Cm), affirm the trend that increasing pressure magnifies the effect of the jet.

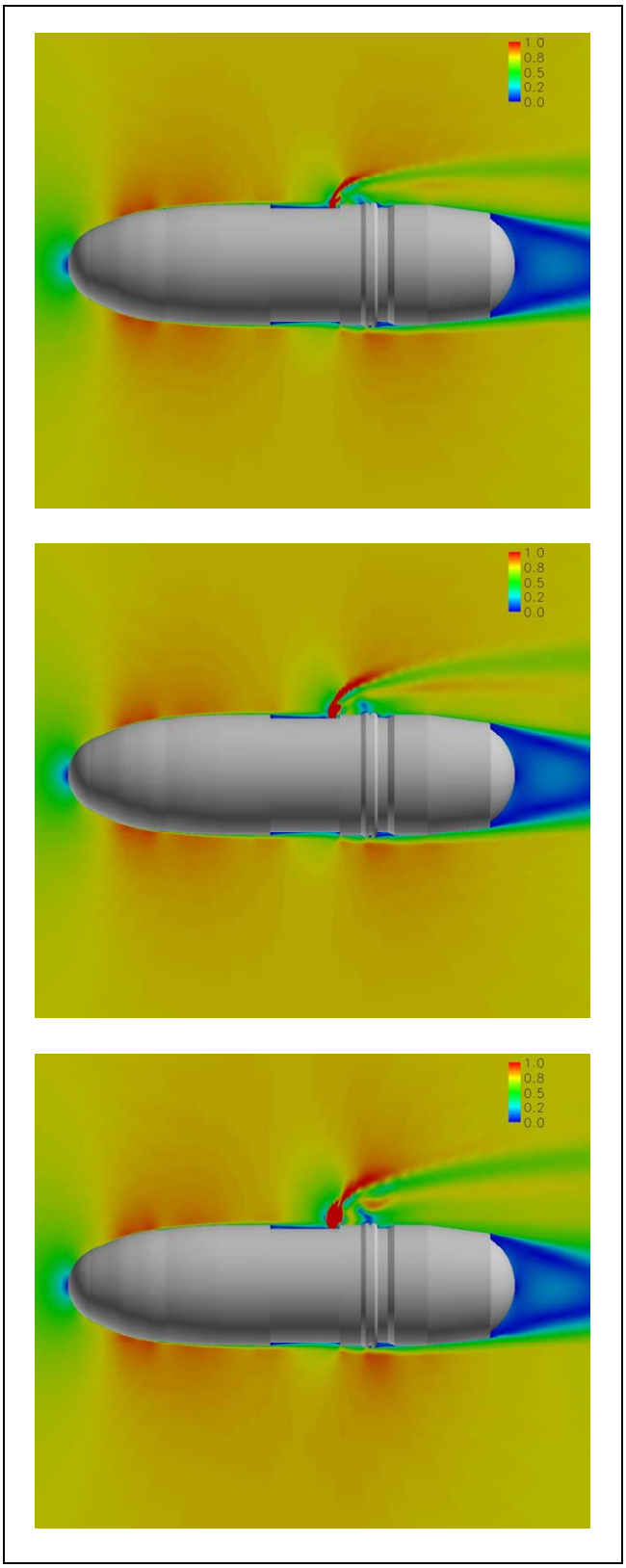

Figure 8. Mach contours for various jet pressures: 3, 6, and 12 atm (top to bottom).

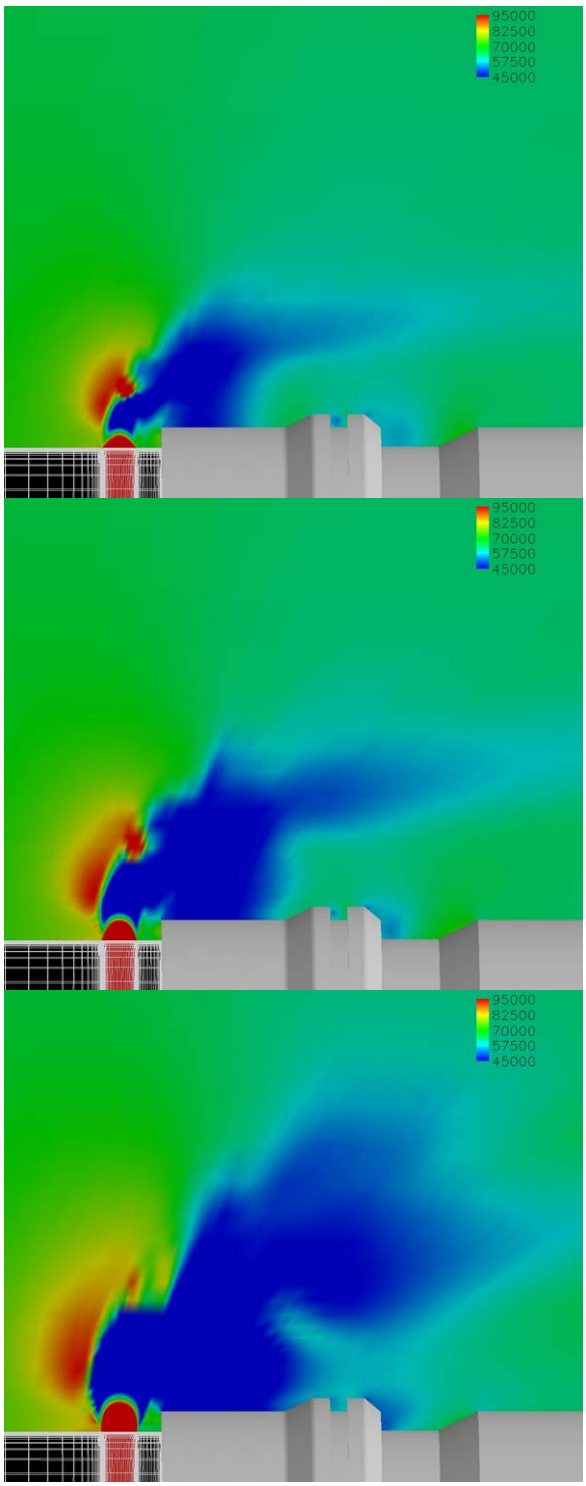

Figure 9. Expanded view of pressure contours for various jet pressures: 3, 6, and 12 atm (top to bottom).

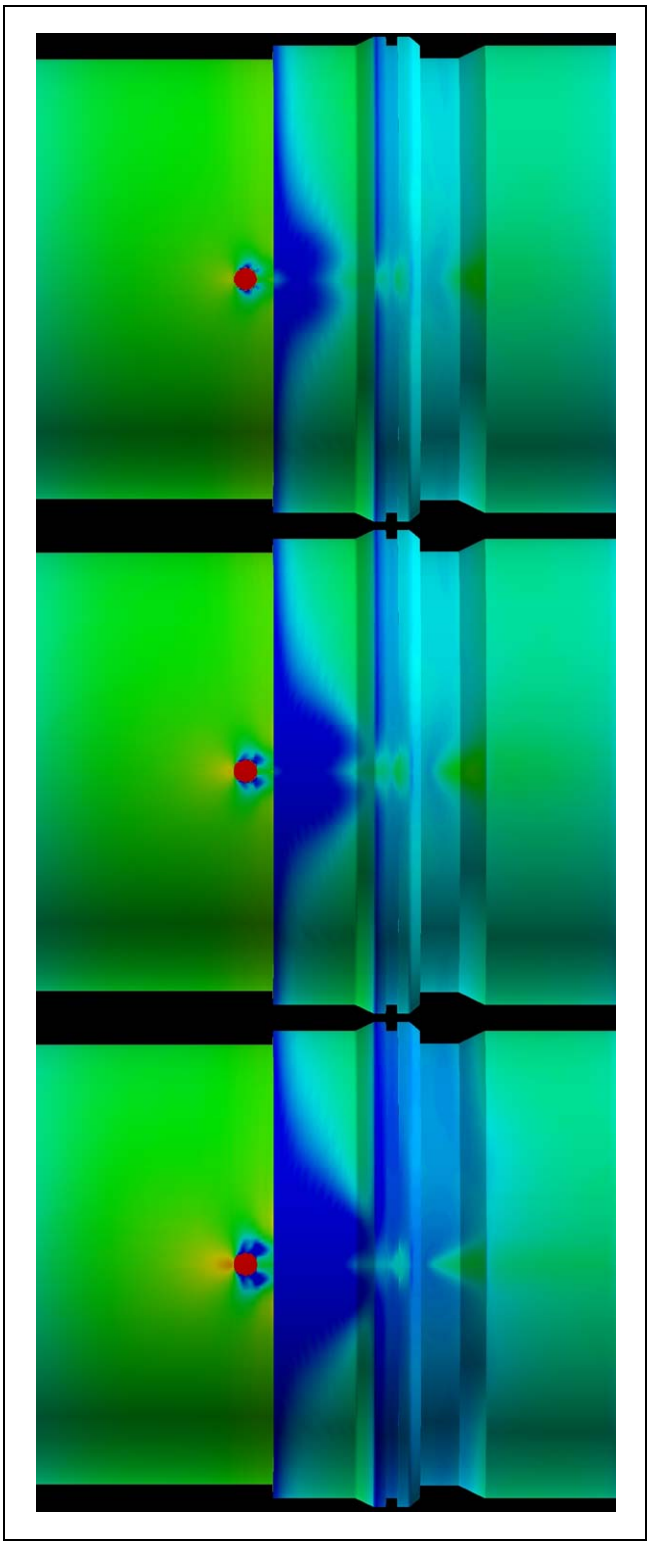

Figure 10. Expanded view of surface pressure contours for various jet pressures: 3, 6, and 12 atm (top to bottom).

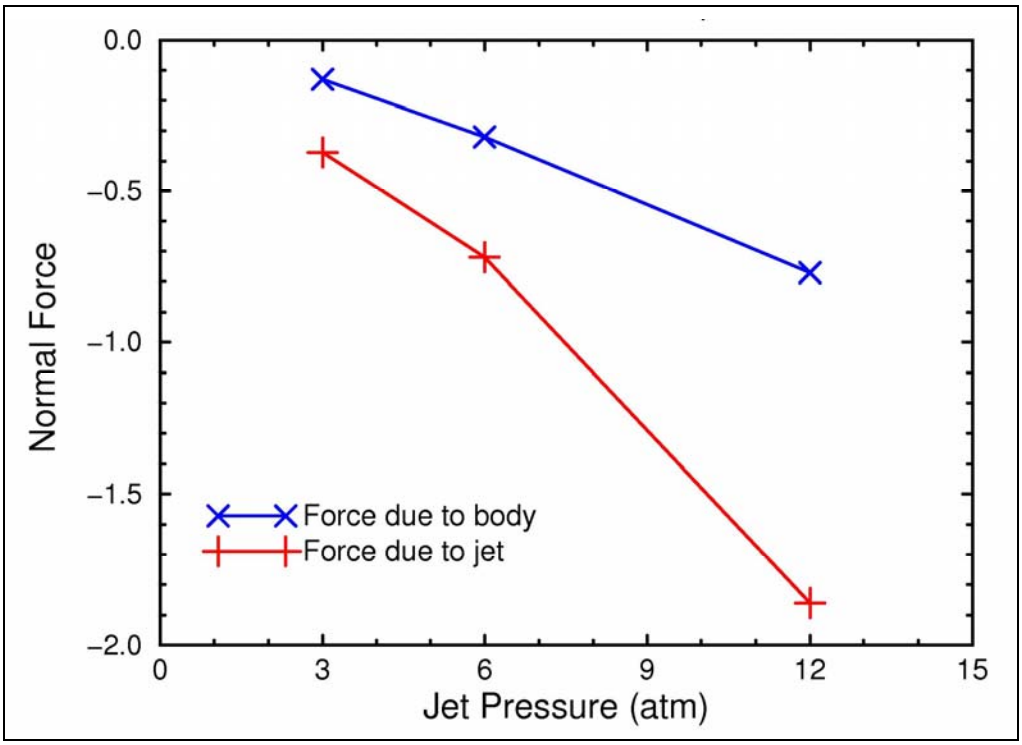

Figure 11. CFD++ results for normal force.

Table 1. Computed values for normal force.

Jet	3 atm	6 atm	12 atm
Fz - body	–0.13	–0.32	–0.77
Fz - jet	–0.37	–0.72	–1.86

Table 2. Computed aerodynamic coefficients.

Model	CX	CN	Cm
Baseline, no cavity	0.156	0.0	0.0
With cavity, jet off	0.149	0.0	–0.001
With cavity, jet = 3 atm	0.149	–0.007	–0.004
With cavity, jet = 6 atm	0.147	–0.017	–0.009
With cavity, jet = 12 atm	0.151	–0.049	–0.033

5. Summary and Conclusions

Numerical computations using viscous Navier-Stokes methods were performed to predict the flow field and aerodynamic coefficients of a 25-mm projectile configuration, with and without a jet cavity, under wind tunnel conditions. Full 3-D computations were performed using a two-equation realizable k-ε turbulence model. Computational results were obtained for these models at Mach number 0.756, alpha 0°, and jet pressures of 3, 6, and 12 atm. Numerical results show the qualitative features of the symmetry plane for the various jet pressures. Force and moment data have been obtained from the computed solutions. Although a stronger jet has an increasing effect on normal force (CN) and pitching moment (Cm), it appears to have little effect on drag (CX).

6. References

1. Sahu, J.; DeSpirito, J.; Edge, H.; Silton, S.; Heavey, K. Recent Applications of Structured and Unstructured Grid Techniques to Complex Projectile and Missile Configurations. *Proceedings of the Eight International Grid Generation and Computational Field Simulations*, Honolulu, HI, June 2002.

2. Peroomian, O.; Chakravarthy, S.; Goldberg, U. *A 'Grid-Transparent' Methodology for CFD*; AIAA Paper 97-07245, 1997.

3. Peroomian, O.; Chakravarthy, S.; Palaniswamy, S.; Goldberg, U. *Convergence Acceleration for Unified-Grid Formulation using Preconditioned Implicit Relaxation*; AIAA Paper 98-0116, 1998.

4. Pulliam, T. H.; Steger, J. L. On Implicit Finite-Difference Simulations of Three-Dimensional Flow. *AIAA Journal* **1982**, *18* (2), 159–167.

5. Silton, S. I.; Guidos, B. J.; Plostins, P. *Objective Crew-Served Weapon (OCSW) 25-mm Projectile Aerodynamics Obtained From Spark Range Firings*; ARL-TR-3299; U.S. Army Research Laboratory: Aberdeen Proving Ground, MD, September 2004.

6. Pointwise, Inc. *GRIDGEN Version 15 On-line User's Manual*; Bedford, TX, 2005.

NO. OF COPIES	ORGANIZATION
1 (PDF ONLY)	DEFENSE TECHNICAL INFORMATION CTR DTIC OCA 8725 JOHN J KINGMAN RD STE 0944 FORT BELVOIR VA 22060-6218
1	US ARMY RSRCH DEV & ENGRG CMD SYSTEMS OF SYSTEMS INTEGRATION AMSRD SS T 6000 6TH ST STE 100 FORT BELVOIR VA 22060-5608
1	DIRECTOR US ARMY RESEARCH LAB IMNE ALC IMS 2800 POWDER MILL RD ADELPHI MD 20783-1197
3	DIRECTOR US ARMY RESEARCH LAB AMSRD ARL CI OK TL 2800 POWDER MILL RD ADELPHI MD 20783-1197

ABERDEEN PROVING GROUND

1	DIR USARL AMSRD ARL CI OK TP (BLDG 4600)

NO. OF COPIES ORGANIZATION

1 COMMANDER
US ARMY TACOM ARDEC
AMSRD AAR AEM A
H HUDGINS
BLDG 95
PICATINNY ARSENAL NJ 07806-5000

1 COMMANDER
US ARMY TACOM ARDEC
AMSRD AAR AEM A
A FARINA
BLDG 95
PICATINNY ARSENAL NJ 07806-5000

1 COMMANDER
US ARMY TACOM ARDEC
AMSRD AAR AEM A
J GRAU
BLDG 95
PICATINNY ARSENAL NJ 07806-5000

1 COMMANDER
US ARMY TACOM ARDEC
AMSRD AAR AEM A
W KOENIG
BLDG 95
PICATINNY ARSENAL NJ 07806-5000

1 COMMANDER
US ARMY ARDEC
SFAE AMO MAS LC
P VALENTI
BLDG 354
PICATINNY ARSENAL NJ 07806-5001

1 NAVAL AIR WARFARE CTR
D FINDLAY
MS 3 BLDG 2187
PATUXENT RIVER MD 20670

1 COMMANDER
US ARMY ARDEC
SFAE AMO CAS MS
P J BURKE
BLDG 162S
PICATINNY ARSENAL NJ 07806-5000

1 ARROW TECH ASSOC
W HATHAWAY
1233 SHELBURNE RD STE D8
S BURLINGTON VT 05403

NO. OF COPIES ORGANIZATION

1 AEROPREDICTION INC
F MOORE
9449 GROVER DR STE 201
KING GEORGE VA 22485

1 ALLEGANY BALLISTICS LAB
D J LEWIS
210 STATE RT 956
ROCKET CENTER WV 26726

1 KLINE ENGRG CO INC
R W KLINE
27 FREDON GREENDEL RD
NEWTON NJ 07860-5213

1 GOODRICH ACTUATION SYS
T KELLY
100 PANTON RD
VERGENNES VT 05491

1 GEORGIA INST TECH
DEPT AEROSPACE ENGRG
M COSTELLO
270 FERST ST
ATLANTA GA 30332

1 COMMANDER
US ARMY TACOM ARDEC
AMSRD AAR AEM A
G MALEJKO
BLDG 95
PICATINNY ARSENAL NJ 07806-5000

1 COMMANDER
US ARMY ARDEC
AMSRD AAR AEP E
D CARLUCCI
BLDG 94
PICATINNY ARSENAL NJ 07806-5000

1 COMMANDER
NAVAL SURFACE WARFARE CTR
CODE 420
A WARDLAW
INDIAN HEAD MD 20640-5035

1 PRODUCT MGR SMALL AND MED
CALIBER AMMO
SFAE AMO MAS SMC
R KOWALSKI
BLDG 354
PICATINNY ARSENAL NJ 07806

NO. OF
COPIES ORGANIZATION

1 PM MAS
SFAE AMO MAS
PICATINNY ARSENAL NJ 07806-5000

1 PM CAS
SFAE AMO CAS
PICATINNY ARSENAL NJ 07806-5000

3 US ARMY AMRDEC
AMSAM RD SS AT
R W KRETZSHMAR
L AUMAN
E VAUGHN
REDSTONE ARSENAL AL 35898-5000

ABERDEEN PROVING GROUND

12 DIR USARL
AMSRD ARL WM
J SMITH
AMSRD ARL WM B
M ZOLTOSKI
AMSRD ARL WM BD
B FORCH
AMSRD ARL WM BC
P PLOSTINS
M CHEN
J DESPIRITO
B GUIDOS
K HEAVEY
J SAHU
S SILTON
P WEINACHT
AMSRD ARL WM BF
W OBERLE